5 Electronic Structure, Exchange and Magnetism in Oxides

D. Khomskii

Laboratory of Solid State Physics, Groningen University,
Nijenborgh 4, 9722 AG Groningen,
The Netherlands

5.1 Introduction

Magnetic oxides are a curious class of materials with good prospects for applications in spin electronics. These materials exhibit a wide variety of magnetic properties (e.g. ferro-, ferri- and antiferromagnetic structures) as well as diverse transport properties including good insulators, systems with insulator–metal transitions, materials with "bad metallic" conductivity, good conductors and superconductors.

Typically in these materials the same electrons are responsible for both the magnetic and electric properties, so a strong interdependence of these characteristics should be seen. Indeed this is what is observed experimentally in many systems of this class. The most spectacular effect of this type is probably the "colossal magnetoresistance" (CMR) – the term coined recently, mostly for the effects observed in doped manganites [1]. This term may be also applied to some other compounds, e.g. EuO, see e.g. [2], in which the effect is sometimes much stronger than in the conventional manganites.

There are a number of textbooks, monographs [3,4] and review articles [5,6,7] in which the basic physics of the transition metal oxides are described. In this short chapter I will present a summary of the main concepts and notions used in describing the structure and properties of transition metal oxides. Special attention will be paid to the question when should *ferromagnetic* order be expected in oxides, and what is the relationship between the type of magnetic ordering and transport properties (notably resistivity) of magnetic oxides.

5.2 Transition Metal Ions in Crystals

Isolated ions with partially filled $3d$-shells have 5-fold degenerate orbitals ($l = 2$, $(2l+1)$-degenerate levels), in which we can put up to 10 electrons ($2 \times (2l+1)$). The filling of these levels follows Hund's first rule: to minimize the Coulomb repulsion energy, electrons form a state with the maximum possible spin. Thus for example the ion $V^{3+}(d^2)$ should have spin $S = 1$; $Mn^{2+}(d^5)$ a spin $S = \frac{5}{2}$ etc.

When a transition metal (TM) ion is put into a crystal, the spherical symmetry of an isolated ion is reduced, and consequently some of the orbital degeneracy is lifted. This is called the splitting of levels due to a crystal field (CF).

M.J. Thornton and M. Ziese (Eds.): LNP 569, pp. 89–116, 2001.

The modification of the $3d$-level can be considered step by step by gradually reducing the symmetry of the surroundings. If for example a TM ion is put into a cubic crystal field (see Fig. 5.1), the 5-fold orbitally degenerate levels are split as shown in Fig. 5.2: three levels go down in energy, forming triply degenerate t_{2g}-levels, and two degenerate e_g-levels go up. The splitting of these levels Δ_{CF} is sometimes called $10\,Dq$, especially in chemical literature.

The splitting of these levels can be understood by examining the form of the d-wave functions for the e_g orbitals:

$$\begin{aligned} d_{x^2-y^2} &= \tfrac{1}{\sqrt{2}}(x^2 - y^2) \\ d_{z^2} &= \tfrac{1}{\sqrt{6}}(2z^2 - x^2 - y^2)\,, \end{aligned} \tag{5.1}$$

i.e. they have an electron density directed towards the negatively charged ions surrounding the TM ions, see Fig. 5.3. These ions are often called ligands, and the resultant crystal field splitting of d-levels is called a ligand field.

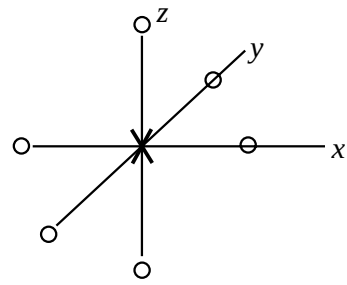

Fig. 5.1. × – transition metal ion; ○ – negative ligand ions (e.g. oxygen)

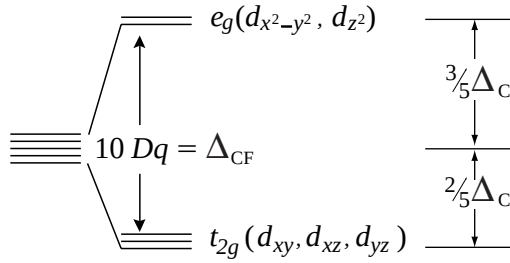

Fig. 5.2. Splitting of a 5-fold orbitally degenerate d-level of an isolated ion in an octahedral crystal field of Fig. 5.1.

In contrast the three t_{2g} orbitals have lobes directed along diagonals in between the ligands, as in Fig. 5.4.

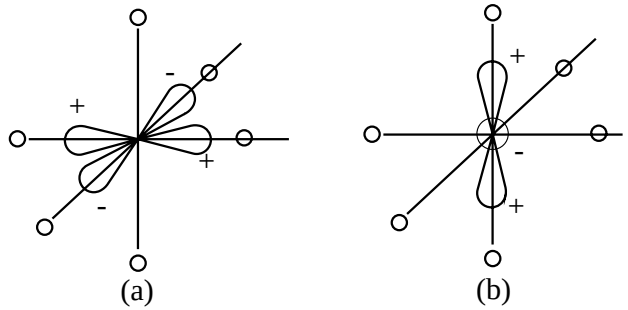

Fig. 5.3. The shape of the e_g-wave functions: (a) $d_{x^2-y^2}$-orbital; (b) $-d_{z^2}$-orbital

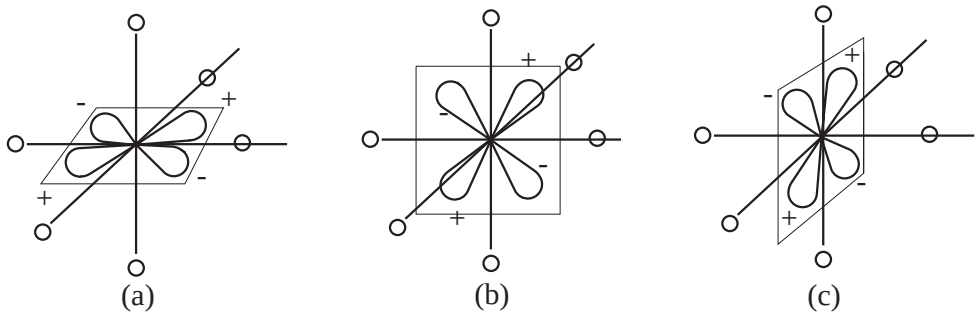

Fig. 5.4. The shape of the t_{2g}-wave functions: (a) d_{xy}; (b) d_{xz} and (c) d_{yz}-orbitals

As seen from Figs. 5.3 and 5.4, the electron density in the e_g-orbitals is directed towards the negatively charged ligands, whereas those in t_{2g}-levels in between them. As a result the e_g-orbitals will experience a stronger Coulomb repulsion with ligands which raises their energies compared to those of the t_{2g}-levels. These simple considerations explain the crystal field splitting shown in Fig. 5.2. Note also that there are different signs of the corresponding lobes of d-functions, marked in Figs. 5.3 and 5.4. These are irrelevant for the Coulomb interaction with ligands giving a point-charge contribution to the CF, but play an important role further on.

There exists another contribution to the CF splitting besides the point charge contribution described above. This is the so called covalency contribution, due to a hybridization of the d-orbitals of the TM ion with the p-orbitals of the ligands (oxygen) as illustrated in Fig. 5.5. Due to this hybridization a mixing of these orbitals occurs, which causes the splitting of the d and p levels. It can easily be seen that the e_g-orbitals have a rather large overlap and hence a strong hybridization with the p-orbitals of oxygen occurs (directed towards the TM ion) leading to the so-called σ-orbitals, see Fig. 5.6. Consequently the mixing of e_g- and p-orbitals will be strong, and gives a corresponding upward shift of the e_g-levels,

$$\delta E_{e_g} \sim \frac{t_{pd\sigma}^2}{\Delta} \,. \tag{5.2}$$

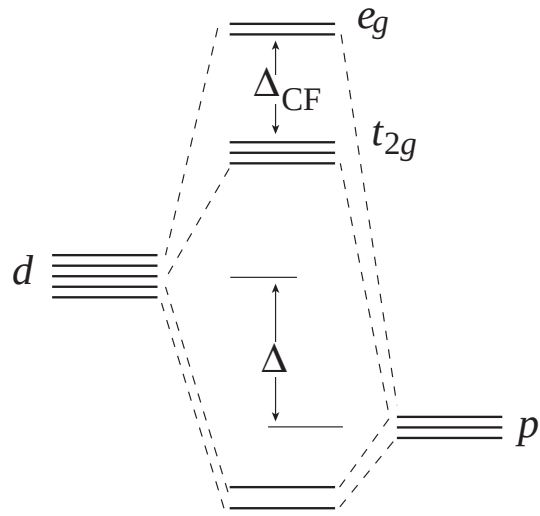

Fig. 5.5. The hybridization of d-levels of the TM ions and p-levels of the ligand leading to the repulsion of levels and splitting of t_{2g} and e_g-levels.

This shift can be estimated by perturbation theory, assuming the p–d hybridization (hopping matrix element) between the e_g- and p-orbitals $t_{pd\sigma}$ is small compared with the initial splitting of d- and p-levels Δ, see Fig. 5.5.

Similar considerations show that the hybridization of the t_{2g}-orbitals with the corresponding p-orbitals of the ligands is smaller than that of e_g-orbitals. Indeed, as seen clearly from Fig. 5.4, the t_{2g}-orbitals are orthogonal to the p-orbitals and

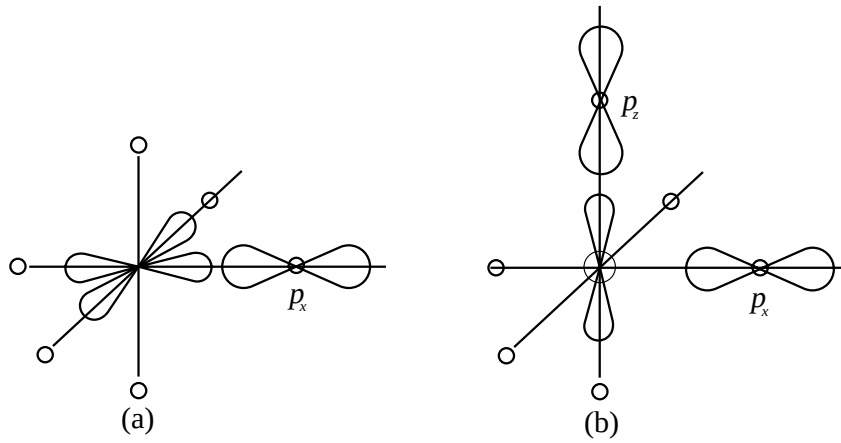

Fig. 5.6. Strong overlap and hybridization of $d_{x^2-y^2}$ (a) and d_{z^2} (b) orbitals with the corresponding p_x and p_z orbitals (σ-orbitals of ligands)

directed towards the TM ions (here the signs of the t_{2g}-wave functions play a crucial role: by symmetry the overlap of p_σ-orbitals with the t_{2g}-orbitals is zero as shown in Fig. 5.6). The remaining overlap between t_{2g} orbitals and p-orbitals shown in Fig. 5.7 is known as π-hybridization. This overlap is permitted by

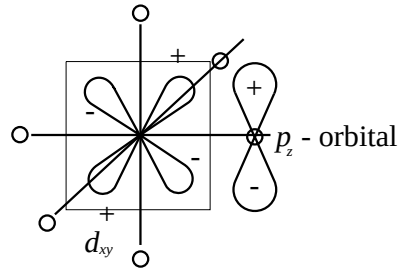

Fig. 5.7. An overlap and hybridization between one of the t_{2g}-orbitals (d_{xz}) with the corresponding p-orbitals (p_z) of a ligand (π-hybridization)

symmetry, but it is smaller than the σ-overlap of e_g-orbitals shown in Fig. 5.6. Since the t_{2g}–p mixing is weaker and the upward shift of the t_{2g}-levels shown in Fig. 5.5 is smaller, then due to the point-charge contribution described above, the e_g levels in a CF are higher in energy than the t_{2g}-levels. Thus both of these contributions to the CF, Coulomb repulsion with ligands and p–d hybridization, in typical cases lead to the same consequence: the splitting of d-levels in a cubic (octahedral) crystal field with the form shown in Fig. 5.2. Typical values of the splitting between t_{2g}- and e_g-levels in TM oxides are $\Delta_{CF}(= 10Dq) \simeq 1$–$2\,\mathrm{eV}$.

Now, using the rule (Hund's rule) formulated above, the ground state of a TM ion may be understood. From the formal valence of a TM in a given compound, the number of d-electrons left on the ion is found, and these electrons may be put in the CF-split levels of Fig. 5.2 one after another following Hund's rule, i.e. putting as many electrons with parallel spins as possible.

So, supposing the total number of d-electrons $n_d \lesssim 3$, then simply the total spin of the ion will be $S = n_d/2$ (we ignore for a while the question of remaining orbital degeneracy, see Sect. 5.3 below). However, if we have four d electrons ($n_d = 4$), a problem may arise. If the fourth electron is placed with the spin parallel to those of the first three electrons, (i.e. according to Hund's rule), then we should place it on a higher-lying e_g-level, see Fig. 5.8a, which costs us an energy Δ_{CF}. Alternatively, the fourth electron could be put on one of the lower t_{2g}-levels; but in this case because of the Pauli principle it should have the opposite spin, i.e. we have to violate Hund's first rule.

Both of these situations are met in practice. The first one leads to the so-called high-spin state of a TM ion, whereas the second one to the low-spin state. As seen from Fig. 5.8, the relative stability of one state with respect to another is determined by the ratio of the CF splitting Δ_{CF} and the Hund's rule stabilization energy (which may be described as an on-site ferromagnetic exchange interaction $-J_H \sum_{\alpha,\beta} \boldsymbol{S}_{i\alpha}\boldsymbol{S}_{i\beta}$, where i is the site index and α, β are

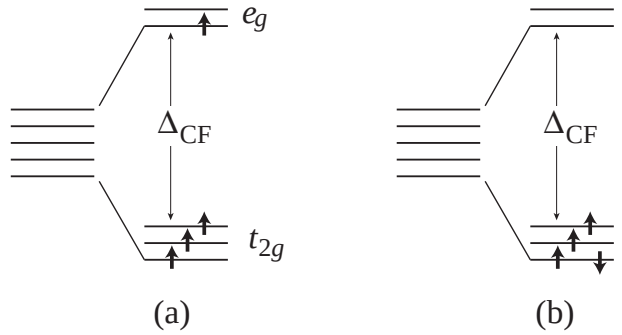

Fig. 5.8. High-spin state (a) and low-spin state (b) of an ion with 4 d-electron

indices of different d-orbitals[1]). If $\Delta_{CF} > J_H$ (or rather larger than the total Hund's rule stabilization energy, which for the case shown in Fig. 5.8 will be $3J_H$, the difference in the number of pairs of parallel spins between the configurations in Fig. 5.8a and 5.8b), then it would be favourable to form a low-spin state, occupying the lowest CF levels at the expense of Hund's rule exchange. In the opposite case the high-spin state will be stabilized.

In most cases the TM oxides have high-spin states (this is the case for $Mn^{3+}(d^4)$ whose configuration corresponds to that of Fig. 5.8a). However there are notable exceptions. The ionic states of $Co^{3+}(d^6)$, Ni^{3+} (d^7) and Ru^{4+} (d^4) are often low level spin ones. Also by changing the parameters such as tempera-

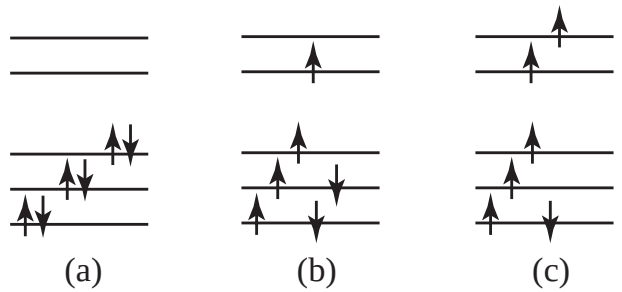

Fig. 5.9. Different possible electronic configurations of ions Co^{3+} and Fe^{2+} (d^6): (a) low-level spin state; (b) intermediate spin state; (c) high-spin state

ture, pressure and composition of the material different spin states may appear, even real phase transitions as the material crosses over from one state to another may occur. This may be the situation in $LaCoO_3$ [3] (for which even a more complicated situation may exist, with the stabilization of an intermediate-

[1] Strictly speaking, the Hund's rule stabilization energy is not an ordinary exchange interaction but is due to the difference of the direct Coulomb interaction of electrons on different orbitals; for our purposes this subtle difference is however irrelevant.

spin state [8]). Maybe the most interesting and the most important phenomena of this kind occur in some of the Fe^{2+}-containing compounds (including many biologically important ones): probably the low spin–high spin transition of Fe^{2+} in such compounds plays an important role in functioning of such molecules and compounds, in particular in red blood cells.

5.3 Orbital Degeneracy and Jahn–Teller Effect

Now going one step further and consider what happens when the point symmetry of a TM ion is further reduced. It was already noted (although we put it for a while under the rug) that there may be situations when the detailed occupation of one or another crystal field level is not uniquely determined. For example, which particular t_{2g}-orbitals would be occupied in the $V^{4+}(d^1)$ ion in an octahedral coordination, or which e_g-orbital would the fourth d-electron go into in a high-spin state of $Mn^{3+}(d^4)$, see Fig. 5.8a.

There exists a very powerful and general theorem in quantum mechanics – the Jahn–Teller theorem – which states, crudely speaking, that the only degeneracy permitted in the ground state of any quantum system is the Kramers degeneracy. This is connected with the invariance with respect to time inversion. In simple terms it is the degeneracy of the spin up and down states (in systems without magnetic order). All the other types of degeneracy including orbital degeneracy (in Fig. 5.8a) are forbidden and should be lifted by the corresponding decrease of symmetry which lifts this degeneracy. The essence of this theorem (which, as Teller himself states in the preface to the book on the JT effect, [9], was actually formulated by Landau) is that: there is always a perturbation reducing the symmetry with a linear term representing the splitting of the degenerate levels (an energy gain) and a quadratic term representing the energy loss, see Fig. 5.10. Following from the standard perturbation theory of degenerate levels in quantum mechanics, the energy of the system as a function of perturbation u has indeed the form

$$E(u) = -gu + \frac{Bu^2}{2} \tag{5.3}$$

where the first term is the splitting of degenerate levels, and the second one is, e.g., the elastic energy of a deformation reducing the symmetry.[2]

For example a regular octahedron may be deformed into a tetragonal to lift the cubic symmetry, see Fig. 5.11. From similar considerations to the ones in Sect. 5.2 it can be seen that the local elongation of O_6-octahedra (Fig. 5.11a) decreases the Coulomb energy of the orbital d_{z^2} in comparison with $d_{x^2-y^2}$, whereas a local compression of the octahedra (Fig. 5.11b) decreases the energy of the other orbital, $d_{x^2-y^2}$.

[2] There may appear important complications in case of isolated JT centers: due to quantum effects there may occur tunneling between the states in the right and the left minima in Fig. 5.10. This gives rise to so-called vibronic effects, considered in detail e.g. in [9]. In concentrated systems which we consider here, these effects are usually not very important, and we will not discuss them in what follows.

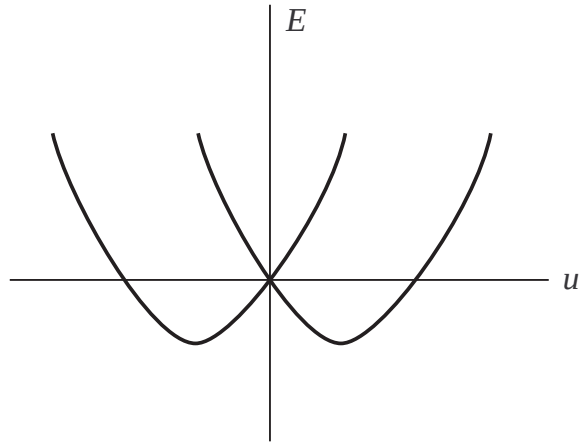

Fig. 5.10. The change of the total energy of a system with two degenerate levels as a function of perturbation (deformation) u decreasing the symmetry and lifting the degeneracy

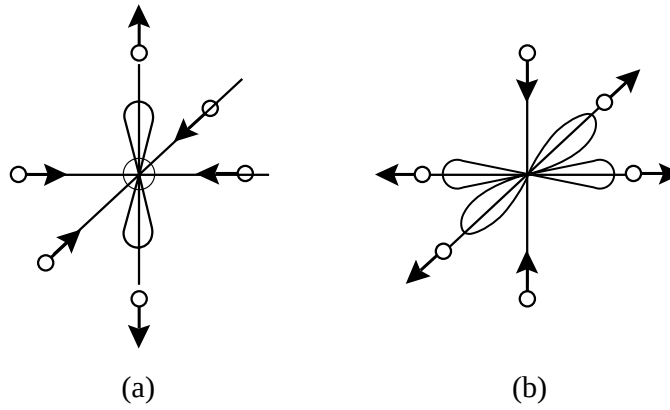

Fig. 5.11. Tetragonal deformation of O_6 octahedra stabilizing one particular orbital: (a) Elongation, stabilizing d_{z^2}-orbital; (b) Compression, stabilizing $d_{x^2-y^2}$-orbital

This is the essence of the Jahn–Teller theorem in application to the transition metal ions with an orbital degeneracy. As typically the neighbouring TM ions have common ligands (e.g. oxygen), a local JT deformation around one centre interacts with the corresponding deformation of its neighbours, see e.g. Fig. 5.12, giving rise to correlated displacements. Consequently the symmetry of the crystal as a whole is reduced. This usually occurs as a structural phase transition – one of very few types (maybe the only one) of structural phase transitions for which we know for sure their microscopic origin. This is known as the cooperative Jahn–Teller effect (CJTE) or as orbital ordering. Due to the distortion a particular orbital is occupied at each center, this may result in a ferrodistortion, or ferro-

orbital ordering, e.g. when all the octahedra are elongated in one direction; this is the situation in Mn ferrites or in Mn_3O_4. Local deformations are often correlated in an antiferrodistortive fashion (Fig. 5.12); this is known as an antiferro-orbital ordering.

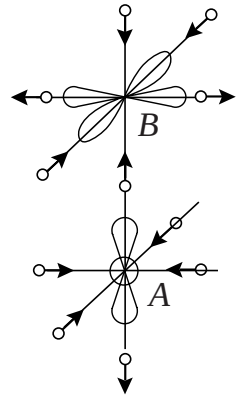

Fig. 5.12. An illustration of correlation of local deformations around neighbouring JT ions A and B, with the corresponding orbital occupation.

Orbital ordering due to the JT effect takes place in many compounds. Typical ions displaying a strong JT effect are $Mn^{3+}(d^4)$, $Cr^{2+}(d^4)$, $Cu^{2+}(d^9)$. In these ions in octahedral surroundings there will be one electron (Mn^{3+}, Cr^{2+}) or one hole (Cu^{2+}) in a doubly degenerate e_g-level. Due to the strong overlap with the p-orbitals of ligands which in their turn strongly depend on the TM–O distance, the splitting of the e_g-levels with a shift of nn oxygens is rather strong, which gives rise to a strong JT coupling. These ions are usually cited as typical JT ions. The JT effect for Cu^{2+} is so strong that Cu^{2+} is never found in a regular octahedron, but always in a strongly elongated one. Local distortion (elongation) around Cu^{2+} can be so strong that one or two apex oxygens can "go to infinity" leaving Cu^{2+} in a 5-fold (pyramid) or 4-fold (square) coordination. Such a coordination is indeed typical for many Cu^{2+} compounds, the best known recent examples being high-T_c cuprates like $YBa_2Cu_3O_7$ etc. Thus the JT nature of Cu^{3+}, even if it may not be directly responsible for high-T_c superconductivity (although the person who discovered it, K. A. Müller, believes that it is), is at least very important for the stabilization of these rather unusual crystal structures.

The JT nature and corresponding orbital ordering is apparently very important in another nowadays popular class of compounds, namely the CMR manganites. The basic undoped compound $LaMnO_3$ contains a strong JT ion, $Mn^{3+}(d^4)$, and indeed there exists in $LaMnO_3$ a structural phase transition at $\sim 800\,K$ caused by the CJTE and orbital ordering. The crude orbital structure of $LaMnO_3$ at room temperature is shown in Fig. 5.13 (the actual occupied orbitals are slightly different). Thus the undoped $LaMnO_3$ has an antiferro-orbital ordering with locally elongated octahedra packed so that the long axes alternate

in the basal plane. Such a distortion is rather typical: it helps to minimize the total strain of a crystal.

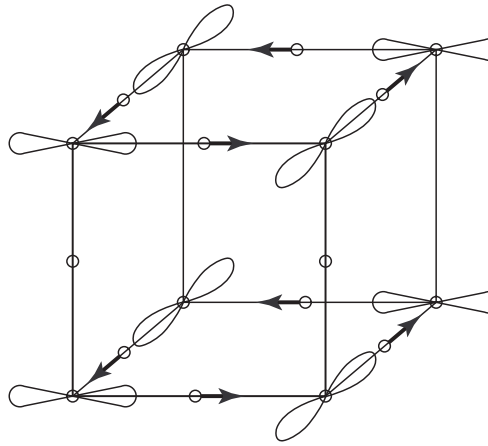

Fig. 5.13. Orbital structure and shifts of oxygens in undoped $LaMnO_3$

As in strong JT ions we are dealing with the double orbital degeneracy and it is convenient to describe the orbital structure by effective pseudospin operators τ so that e.g. the state $\tau^z = +\frac{1}{2}$ corresponds to orbital 1 (e.g. d_{z^2}), and $\tau^z = -\frac{1}{2}$ to orbital 2 ($d_{x^2-y^2}$). An arbitrary linear superposition of orbitals can always be formed, and written as

$$|\theta\rangle = \cos\frac{\theta}{2}|d_{z^2}\rangle + \sin\frac{\theta}{2}|d_{x^2-y^2}\rangle \tag{5.4}$$

(coefficients are written in such a form to guarantee proper normalization of the wave function $|\theta\rangle$). The corresponding states can then be depicted in the $(\tau^z, \tau^x)-$, or θ-plane, see Fig. 5.14. In Fig. 5.14 the state with $|\theta = 0\rangle$ would correspond to $|d_{z^2}\rangle$, $|\theta = \pi\rangle = |d_{x^2-y^2}\rangle$. But what is more interesting, the states obtained from $|d_{z^2}\rangle$, $|d_{x^2-y^2}\rangle$ by the rotation of axes can be marked on this diagram (as in a regular octahedron the directions x, y and z are equivalent). Of course, not only an orbital d_{z^2} extended in the z-direction can be formed, but also equivalent orbitals d_{x^2} and d_{y^2} extended along the x and y-axes (such orbitals are shown in Fig. 5.13). In Fig. 5.14 these orbitals would correspond to $|\theta = \pm\frac{2}{3}\pi\rangle$, and orthogonal orbitals $d_{z^2-x^2}$, $d_{z^2-y^2}$ to $|\theta = \pm\frac{1}{3}\pi\rangle$. Thus in this language the orbital structure of $LaMnO_3$ (shown in Fig. 5.13) would correspond to a "canted" τ-antiferromagnetism, with one sublattice having pseudospins at an angle $\theta = \frac{2}{3}\pi$ and another at $\theta = -\frac{2}{3}\pi$ (actual angles of sublattices in $LaMnO_3$ are somewhat different, closer to $\simeq \pm 97°$).

Up to now only the strong JT ions with double e_g-degeneracy have been discussed. There are, however, many materials with triply-degenerate t_{2g}-orbitals:

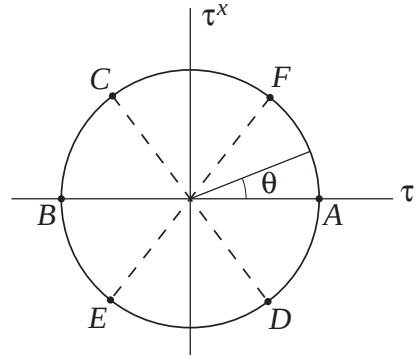

Fig. 5.14. τ^z–τ^x plane in which all the possible e_g states can be conveniently visualized. In this diagram the point A ($\theta = 0$) corresponds to the orbital d_{z^2}, B—to $d_{x^2-y^2}$, C ($\theta = \frac{2}{3}\pi$)—to d_{x^2}, D—to $d_{z^2-y^2}$, E ($\theta = -\frac{2}{3}\pi$)—to d_{y^2} and F—to $d_{z^2-x^2}$

for example compounds of $V^{4+}(d^1)$ or $V^{3+}(d^2)$. Such materials also display features typical for the JT effect, however, there is one important difference between the t_{2g}-ions compared with the e_g-ions. For the latter the real orbital moment is quenched, for t_{2g}-ions there exists a nonzero orbital moment $l_{eff} = 1$ and correspondingly there is a spin–orbit interaction $\lambda \boldsymbol{l} \cdot \boldsymbol{s}$. This interaction can by itself lift the orbital degeneracy, and in typical situations it leads to a distortion (which in this case is usually called magnetostrictive distortion) opposite in sign to the one caused by the JT effect. Thus different compounds containing t_{2g} ions may distort along different "routes": in some the ground state is determined by the JT distortion, but others develop "along the $\boldsymbol{ls}$-route" and have a magnetostrictive distortion of the opposite sign. The second class of compounds typically contains materials with $Co^{2+}(d^7)$ and high-spin $Fe^{2+}(d^6)$ ions. The characteristic feature of compounds in which $\boldsymbol{ls}$-coupling dominates and determines the ground state, is a decrease of symmetry and a lifting of the degeneracy occurring simultaneously with the magnetic ordering. In typical systems where the JT effect dominates, this happens independently and usually at higher temperatures than any magnetic ordering.

There are a number of interesting features in magnetic oxides containing JT ions, for further details see [6] and [10]. In the next section the mechanisms and the main features of the exchange interaction in oxides are discussed in which the orbital structure of corresponding ions plays a crucial role.

5.4 Exchange Interaction in Magnetic Insulators

Predominantly the electronic structure of isolated TM ions in crystals has been considered, with their attributes in concentrated systems arising from an interaction between ions. One such effect already mentioned above is the cooperative Jahn–Teller effect, or orbital ordering. More importantly in these systems are the magnetic interactions leading to some kind of long-range magnetic ordering,

and the possibility of electron transfer from site to site. This effect is responsible for the transport properties seen in corresponding materials.

The simplest description of these properties should include the possibility of electron hopping as well as the effect of the Coulomb interaction between electrons. For a more complex model such details as the orbital structure of the corresponding ions should be taken into account. The d-electrons in crystals are described by the so-called Hubbard model:

$$H = -\sum t_{ij} c^+_{i\sigma} c_{j\sigma} + U \sum n_{i\uparrow} n_{i\downarrow} \equiv H' + H_0. \tag{5.5}$$

Here the first term describes the hopping of d-electrons from site j to site i, and the second term is the on-site Coulomb repulsion of d-electrons. This nondegenerate Hubbard model ignores such complications as a possible orbital degeneracy, but it is sufficient for the description of both insulating and metallic states of our system as well as for formulating the basics of the exchange interaction in magnetic insulators.

As is well known, for weak interaction $U \ll t$ the model (5.5) describes the metallic state, with the band dispersion

$$H' = \sum \varepsilon_k c^+_{k\sigma} c_{k\sigma}\,, \qquad \varepsilon_k = -2t(\cos k_x + \cos k_y + \cos k_z)\,. \tag{5.6}$$

(The simplest tight-binding approximation with only nearest neighbour hopping is used and the spectrum is written for a simple cubic lattice.) In this case the system would be metallic even for an exactly half-filled band with one electron per site, $n = 1$, independent of the distance between corresponding sites.

It is clear however that for large enough distance between sites, which means small hopping matrix element t, and for $n = 1$, the ground state should be insulating with electrons localized each at its site. This state is called a Mott or a Mott–Hubbard insulator, and it is due to the second term in the Hamiltonian (5.5), the on-site Coulomb repulsion U. If the overlap of the nn electron wave functions is small enough so that $t \ll U$, care should be taken with the second term in (5.5) which should be minimized if there is exactly one electron per site and electrons are forbidden to hop onto the already occupied site. As a result the ground state electrons will be localized, and creation of charge excitations (transfer of an electron from its site to another one) would cost an energy U (the repulsion of the transferred electron with the one already existing at this site). The energy gain in this process would be $\sim t$ (both the extra electron and the hole left at the first site can now move through the crystal and gain corresponding kinetic energy of the order of their bandwidth (5.6), i.e. $\sim t$), but if $U \gg t$ the energy loss of this process $\sim U$ exceeds the energy gain $\sim t$, so that the material would remain an insulator, with an energy gap $E_g \sim U - t$. Essentially, this is the physics of strongly correlated (strongly interacting) electron systems.

There are a number of interesting and to a large extent still unsolved problems in the physics of strongly correlated electron systems, see e.g. [11,12], but these cannot be discussed here in detail. Therefore, we will concentrate mostly on

the properties of such systems for a simple case, i.e. for an integral number of electrons per site (e.g. $n = 1$) and for the case of a strong interaction $U \gg t$.

For $n = 1$ and $U \gg t$ the ground state of our system is an insulator. Thus there exists at each site a localized electron, i.e. a localized magnetic moment with $s = \frac{1}{2}$. These moments of course somehow interact with one another so that some kind of magnetic ordering should be established and spin degeneracy would be lifted at low temperatures; otherwise the Nernst theorem would be violated.

The main term of the Hamiltonian (5.5), the second term, leads to the formation of localized moments but it does not lift this spin degeneracy. However, the first term in (5.5), the electron hopping term, lifts this degeneracy (in second order of perturbation theory in $t/U \ll 1$) and leads to an antiferromagnetic exchange interaction between these localized magnetic moments. This result can be obtained rigorously, see e.g. [13,12], but here we will use a simple form which will be easily generalized later for more realistic cases of orbital degeneracy structure.

Consider two neighbouring sites with either parallel or antiparallel spins shown in Fig. 5.15. Electrons initially localized each at its site want to delocalize

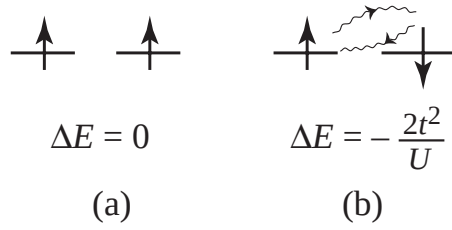

Fig. 5.15. Two neighbouring sites with parallel (a) and antiparallel (b) spins. The energy gain due to virtual hopping of an electron to a neighbouring site is shown

as much as possible by virtual hopping to neighbouring sites; by the Heisenberg uncertainty principle this would decrease their kinetic energy. Such delocalization may be caused by the first term of the Hamiltonian (5.5). In the situation of Fig. 5.15a this process is, however, forbidden by the Pauli principle; on the other hand for the antiparallel spins, Fig. 5.15b, this process is allowed. As a result the first electron hops to a neighbouring site (with the matrix element t), and then back. As usual in second order perturbation theory in quantum mechanics, this decreases the energy of the system, the energy gain being given by $\Delta E = -2t^2/U$ (the term H' in (5.5) acts twice, therefore we have t^2 in the numerator; in the denominator, as usual, the energy of the intermediate state should stand and this is the energy of the repulsion of two electrons at the same site U). The factor of 2 comes from the fact that the left spin can make an "excursion" to the right and the right one to the left.

As a result the configuration with antiparallel spins is preferred relative to the one with the parallel spins. This can be described by the effective exchange

interaction

$$H_{eff} = J \sum \boldsymbol{S}_i \boldsymbol{S}_j \,, \qquad J = \frac{2t^2}{U} \,. \tag{5.7}$$

Virtual hopping of electrons leads to an antiferromagnetic Heisenberg exchange interaction and this type of exchange mechanism is usually called *superexchange* (sometimes also kinetic exchange). This is the main mechanism of exchange interaction in magnetic insulators like transition metal oxides.

5.5 Charge-Transfer versus Mott–Hubbard Insulators

Before discussing the complications introduced by the realistic crystal and orbital structure of materials, one more point should be discussed here. In contrast to the idealized model (5.5), in real materials, e.g. in oxides, usually there are ligands (oxygen ions) between TM ions. Consequently the hopping of d-electrons from site to site (first term in (5.5)) occurs not directly but via oxygen p-orbitals.

In many cases the oxygen p-states can be excluded and this reduces the description to the effective model (5.5); however, this is not always the case. Accordingly all magnetic insulators may be divided into two big groups: Mott–Hubbard insulators for which the description given above applies without any restriction, and charge-transfer insulators in which one should treat oxygen p-states in an apparent way.

The basic general Hamiltonian describing both the d-electrons of the TM and the p-electrons of oxygen has the form

$$H = \sum \varepsilon_d d^+_{i\sigma} d_{i\sigma} + \varepsilon_p p^+_{j\sigma} p_{j\sigma} + t_{pd}(d^+_{i\sigma} p_{j\sigma} + \text{h.c.}) + U n_{di\uparrow} n_{di\downarrow} \,. \tag{5.8}$$

Depending on the ratio of the charge-transfer excitation energy $\Delta = \varepsilon_d - \varepsilon_p$ and the Coulomb repulsion U, a division into two groups can be made.

If the oxygen p-levels lie deep enough, $\Delta \gg U$, the lowest charged excited states are those corresponding to the transfer of a d-electron from one TM site to another:

$$d^n + d^n \longrightarrow d^{n-1} + d^{n+1} \,.$$

This process as described above costs an energy U and for $U \gg t$ gives the Mott–Hubbard insulating state. Still even in this case real hopping occurs via the oxygen p-states, but it can be excluded in perturbation theory, obtaining the effective d–d hopping $t_{dd} = t = t^2_{pd}/\Delta$. This is the d–d hopping t which would enter the effective Hubbard model (5.5) and later the exchange integral (5.7). This is typically seen in oxides of the early transition metals, like Ti and V.

On the other hand there may be situations, where the charge-transfer energy $\Delta = \varepsilon_d - \varepsilon_p$ (the energy necessary to transfer an electron from the filled $2p$-level of O^{2-} to a d-level of a neighbouring TM) is less than U. In this case the lowest charge-carrying excitations will be just these excitations: the transfer of an electron from oxygen to the TM, or the transfer of a hole to an oxygen:

$$d^n p^6 \longrightarrow d^{n+1} p^5 \equiv d^{n+1} \underline{L}$$

(the notation $\underline{L}$ is very often used nowadays and means "ligand hole" – the state with one electron on a ligand – here oxygen – missing).

According to this division we may draw a general phase diagram, the so called Zaanen–Sawatzky–Allen (ZSA) [14] diagram, shown in Fig. 5.16. Many oxides of late 3d-metals (Co, Ni, Cu) belong to this second category, the charge-transfer insulators.

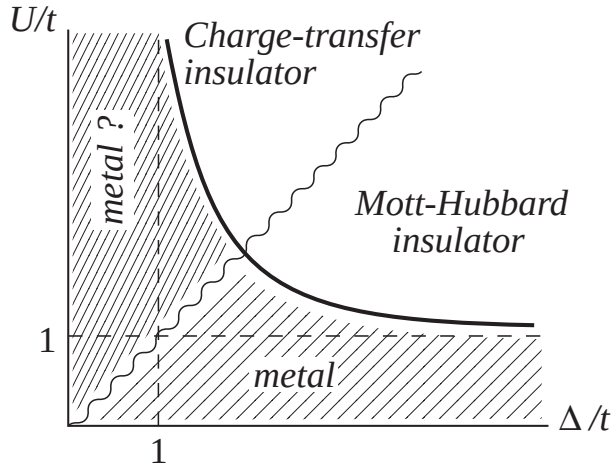

Fig. 5.16. Zaanen–Sawatzky–Allen diagram showing the regions of Mott–Hubbard ($\Delta > U$) and charge-transfer ($\Delta < U$) insulators

If $n = 1$ and the hopping t is small, then even with $\Delta \ll U$ (but $\Delta \gg t$) we would have a similar situation to the one described above: the ground state will still be an insulator with electrons localized at the TM ions and with localized magnetic moments; this is similar to conventional Mott insulators. In the simplest cases such insulators will be antiferromagnetic, with the only difference being the exchange integral J in (5.7) expressed as

$$J = \frac{2t_{pd}^4}{\Delta^2(2\Delta + U_{pp})}\,. \tag{5.9}$$

(Here we take into account the lowest excited states participating in the virtual electron hopping: the electrons that transfer from the oxygen p-shell to the TM d-levels, see Fig. 5.17; we also included the effective repulsion of two p-holes on the same oxygen U_{pp} which contributes to the energy of one of the excited states of Fig. 5.17.) Thus from the point of view of magnetic properties, charge-transfer insulators do not significantly differ from the conceptually simpler Mott–Hubbard insulators, and for our purposes their difference could be ignored. However, it should be realized that there may be differences in these compounds in their excitation spectra, transport properties etc. Further effects

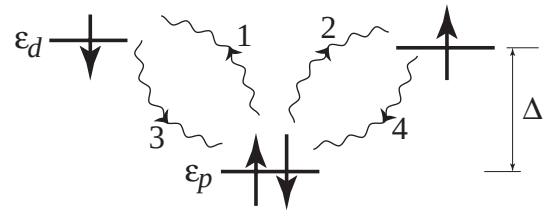

Fig. 5.17. Virtual processes with the hopping of *p*-electrons from oxygen to two neighbouring TM ions giving rise to an effective antiferromagnetic interaction in charge-transfer insulators. The numbers at the wavy lines denote the sequence of virtual transitions

are discussed in detail in Refs. [15,7] and used for the description of some real materials, e.g. CrO_2 in [16].

5.6 Goodenough–Kanamori–Anderson Rules

Until now when discussing the exchange interaction only the simplest case of a nondegenerate *d*-orbital containing one electron has been considered. In reality, as discussed in Sect. 2, *d*-electrons have a rather rich orbital structure: different orientation, different overlap between themselves and with the *p*-states of their ligands and possibly orbital degeneracy. All these details play an important role in determining the corresponding exchange interaction and determine finally the large variety of magnetic properties of TM insulators.

Rules called the Goodenough–Kanamori–Anderson (GKA) rules [3] were formulated in order to predict the observed phenomena.

There are many details and particular cases to consider, so only the main rules are formulated and the general approach explained; however, sometimes the outcome is not clear without detailed calculations. Nevertheless, the general trend is rather straightforward and results from the physics already described in previous sections.

So for the simplest case shown in Fig. 5.18a the localized electrons on two neighbouring TM ions occupy orbitals that are directed towards each other (or overlapping with the same *p*-orbital of the intermediate ligand, Fig. 5.18b). Thus the exchange interaction, according to (5.7) and (5.8) will be rather strong and antiferromagnetic. Note that in a real situation the *dd*-overlap occurs usually via

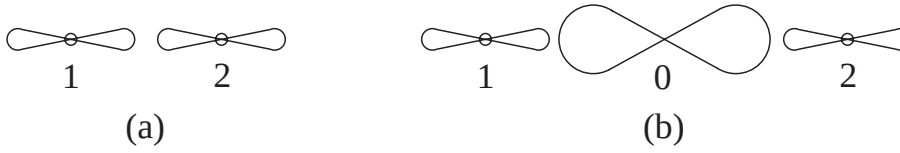

Fig. 5.18. Overlap of *d*-orbitals of two transition metal ions 1 and 2, direct one (a) or via *p*-orbital of the intermediate oxygen O (b)

p-orbitals of intermediate ligands, Fig. 5.18b. In this case the geometry of the corresponding bonds is crucial: the case of Fig. 5.18b represents what we call 180°-exchange (the angle TM 1–O–TM 2 is 180°). *This is the first GKA rule: the* 180° *exchange between filled orbitals (sometimes one speaks about half-filled orbitals, having in mind that there is* **one** *electron at each orbital, not two) is relatively strong and antiferromagnetic.*

Now consider the situation with filled orbitals but with a 90°-exchange path, Fig. 5.19. Likewise in this case we are also dealing with the orbitals (shaded one on TM 1 ion and white on ion TM 2) but interacting via the oxygen with a 90° exchange path 1–O–2. As discussed in the previous section, the actual electron transfer occurs between the d-orbitals of the TM and the p-orbitals of oxygen. It can be easily seen from Fig. 5.19 that two different orthogonal orbitals p_x and p_y overlap with the corresponding d-orbitals of sites 1 and 2. As a result the virtual electron hops as shown in Fig. 5.19b: one electron is transferred from the p_x-

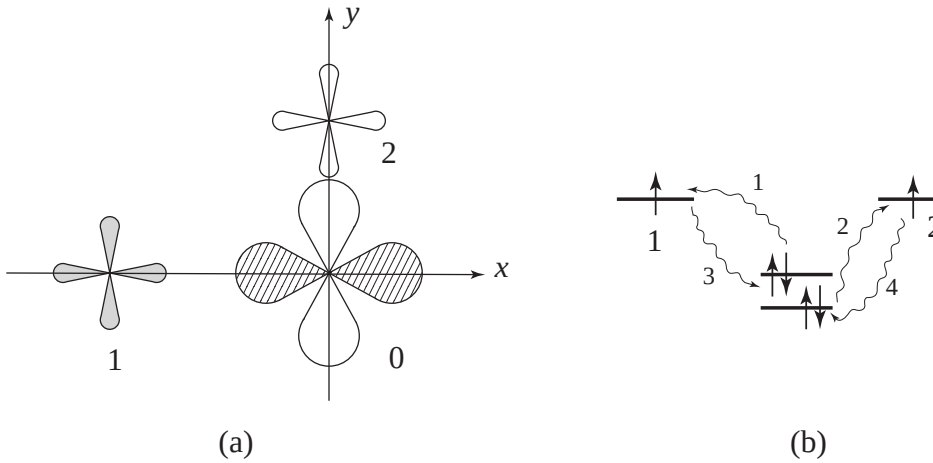

Fig. 5.19. The scheme of 90°-exchange illustrating the second GKA rule. (a) The relevant orbitals at the transition metals 1 and 2 (TM1 and TM2) and oxygen O; (b) Virtual processes with the hopping of p-electrons trom a "corner" oxygen into two neighbouring TM ions giving rise to the ferromagnetic interaction.

orbital to the TM 1 ion, and another electron from a *different* orbital of the same oxygen, p_y, goes into the TM 2 ion. Thus in the excited intermediate state there will be two electrons missing, or two p-holes present, on the oxygen. Depending on the relative spin orientation of TM 1 and TM 2 the remaining p-electrons will be either parallel (the case shown in Fig. 5.19b), or antiparallel. The energy of this intermediate state is in the denominator of the corresponding energy, and as usual the state with the lowest denominator is favoured. Accordingly, to Hund's rule (also valid for the oxygen ion), it is best to have the spins of the two oxygen electrons, or two p-holes, parallel: thus the spins of TM 1 and TM 2 should be

parallel too. As a result of such an exchange process a *ferromagnetic* interaction between the moments of the TM ions 1 and 2 is favoured.

The energy difference between the parallel and antiparallel configurations is

$$J \sim -\frac{t_{pd}^4}{\Delta^2}\left(\frac{1}{2\Delta + U_p - J_H} - \frac{1}{2\Delta + U_p}\right) \simeq -\frac{t_{pd}^4}{\Delta^2(2\Delta + U_p)}\frac{J_H}{(2\Delta + U_p)} \quad (5.10)$$

(cf. (5.9)), i.e. the 90° ferromagnetic exchange would contain a small factor $\sim J_H/(2\Delta + U_p)$. *Thus the second GKA rule reads:* 90°*-exchange between (half)-filled orbitals is* **ferromagnetic** *and relatively weak.*

To illustrate the third and final GKA rule, consider an electron hopping between the *d*-states, as in a simple Hubbard model, not between occupied orbitals, as in Fig. 5.15b or Fig. 5.18, but between an *occupied* and an *empty* orbital. (In real life such hopping goes still through the intermediate ligands but we can skip this detail for a while.) Thus, imagine two TM ions with orbital ordering so that there is no overlap between occupied orbitals, and the only overlap is between an occupied and an empty one, see Fig. 5.20. In this figure the $d_{x^2-z^2}$-orbital (white

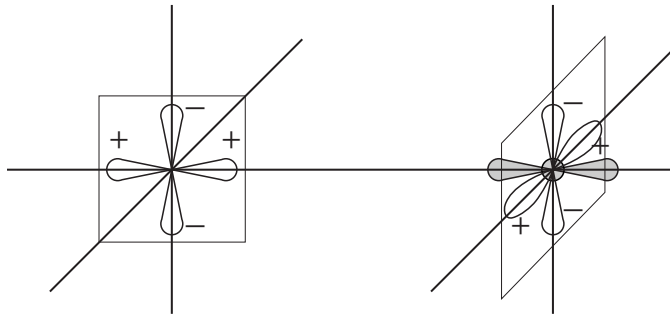

Fig. 5.20. The scheme illustrating the origin of the ferromagnetic exchange for the overlap between occupied and empty orbitals of neighbouring TM ions

one) is occupied at the site 1 and the $d_{y^2-z^2}$-orbital (white) at the site 2. (This orbital occupation is seen in $KCuF_3$, with the only difference being, the orbitals of one *d*-hole in $Cu^{2+}(d^9)$ and not of a *d*-electron are those concerned.) Due to the symmetry of the corresponding wave functions (note the signs in Fig. 5.20!) these orbitals are orthogonal, and there is no hopping between them. However there is a possibility of electron hopping from the occupied $d_{x^2-z^2}$-orbital of the site 1 into an *empty* d_{x^2} (shaded orbital) at the site 2. Such virtual hopping is in principle allowed irrespective of the relative orientation of the spins of the sites 1 and 2. However, as in the previous case, the energies of the intermediate states entering the denominators in second order perturbation theory would differ, cf. Fig. 5.21. In this case, due to Hund's rule, the energy gain in the intermediate state is J_H and the total exchange will be ferromagnetic. Again, as in (5.10), the total exchange constant will be given by the corresponding difference

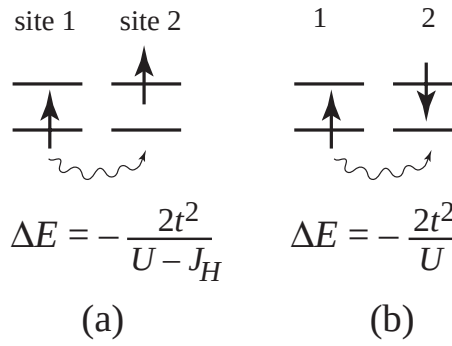

Fig. 5.21. Virtual hoppings from the occupied orbital on site 1 into an empty one on site 2 and corresponding energy gains for the parallel (a) and antiparallel (b) spin orientations

of the energies of the states 5.21a and 5.21b, i.e.

$$J \simeq -\frac{2t^2}{U}\frac{J_H}{U} \,. \tag{5.11}$$

(Taking into account $J_H < U$ and expanding the expression in Fig. 5.21 in J_H/U; typical values for the TM oxides are $J_H \sim 0.8\,\mathrm{eV}$ and $U \sim 3$–$5\,\mathrm{eV}$.) *Thus we justify our third GKA rule: when the exchange is due to an overlap between an occupied and an empty orbital, the resulting exchange is ferromagnetic and relatively weak.*

These main rules will be illustrated by a few examples, for instance, perovskite materials with the basic structure shown in Fig. 5.22. This is probably the simplest feasible structure: magnetic ions form a simple cubic lattice, and the ligands (e.g. oxygen ions) are sitting in between them. The TM ions in this struc-

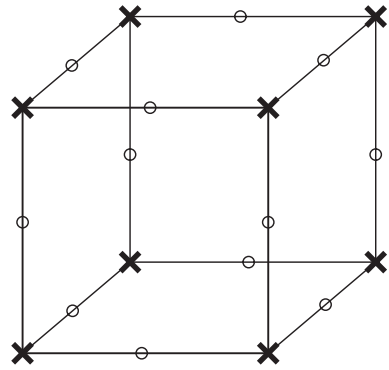

Fig. 5.22. Schematic crystal structure of perovskites; × — transition metal ions; ∘ — oxygen (or other ligand) ions

ture are surrounded by oxygen octahedra, connected by the common corners, so that the superexchange paths TM–O–TM are 180° ones.[3]

Now according to the GKA rules formulated above, when both the e_g-orbitals of the TM ion are occupied, we have an antiferromagnetic *nn* interaction, and as a result the magnetic ordering is of a simple two-sublattice type (the so-called *G*-type antiferromagnetism). This is the situation, e.g., in $KMnF_3$ (Mn^{2+}, d^5), $KNiF_3$ (Ni^{2+}, d^8), $LaFeO_3$ (Fe^{3+}, d^5) etc.

For another example, as already mentioned, $KCuF_3$ contains the typical JT ion $Cu^{2+}(d^9)$ with one hole in a doubly-degenerate e_g-level. In this material the orbital ordering shown in Fig. 5.23 is realized. As explained above, see Fig. 5.20, an exchange interaction in the basal *xy*-plane is relatively weak and *ferromag-*

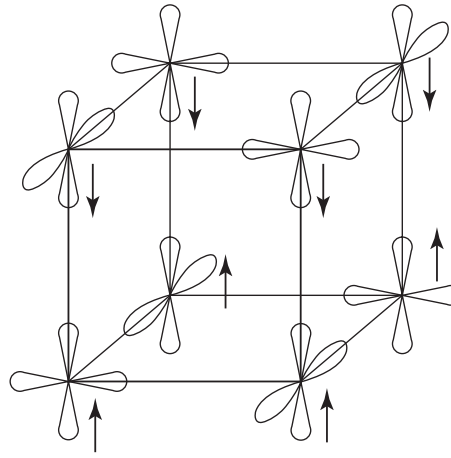

Fig. 5.23. One of two possible types of orbital ordering in $KCuF_3$ (the other one differs by the interchange of the occupied orbitals in the upper *xy*-plane)

netic. On the other hand, along the *z*-direction the lobes of occupied orbitals are directed towards each other, which, according to the first GKA rule, results in a strong antiferromagnetic interaction in this direction. As a result the magnetic structure shown in Fig. 5.23 is obtained: the ferromagnetic *xy*-planes are coupled antiferromagnetically in the *z*-direction (this magnetic structure is called *A*-type antiferromagnetism). Thus, due to a particular orbital ordering, the magnetic structure in a compound close to a cubic one is rather anisotropic. Moreover, as explained, the antiferromagnetic exchange in *z*-direction is much stronger than the ferromagnetic one in *xy*-plane, so in effect $KCuF_3$ has properties of a quasi-one-dimensional antiferromagnet (antiferromagnetic chains in the *z*-direction with weak ferromagnetic coupling between them), and, despite

[3] In reality often MO_6-octahedra are tilted so that the exact angle TM–O–TM is less than 180°. In many cases this has important consequences; for our general discussion however we ignore this complication

being structurally a nearly cubic compound, is one of the best examples of one-dimensional antiferromagnets.

Another very important example is given by the compound $LaMnO_3$, the basis of the CMR materials so popular nowadays. Its orbital structure has been already shown in Fig. 5.13. The application of the GKA rules to this compound is not as straightforward as above (see the detailed discussion in [7]), but the outcome is the same: the type-A antiferromagnetic structure (ferromagnetic planes stacked antiferromagnetically) is seen, with the important difference from $KCuF_3$ being, the ferromagnetic exchange in the basal plane is stronger than the antiferromagnetic one between these planes.

The fact that due to the orbital ordering four of the nearest neighbours out of six have ferromagnetic coupling may be important for the formation of the ferromagnetic state in doped $LaMnO_3$, although usually this is ascribed to the double exchange mechanism, see below. This is definitely important, but it may well be that the factor mentioned above (ferromagnetic coupling due to orbital ordering) also plays some role in it.

In order to illustrate the second GKA rule, many materials with 90°-exchange which gives ferromagnetic interaction may be cited. Probably the simplest examples are provided by the one-dimensional structures containing Cu^{2+}, shown in Fig. 5.24. In these structures the angle Cu–O–Cu is often very close to 90°, and

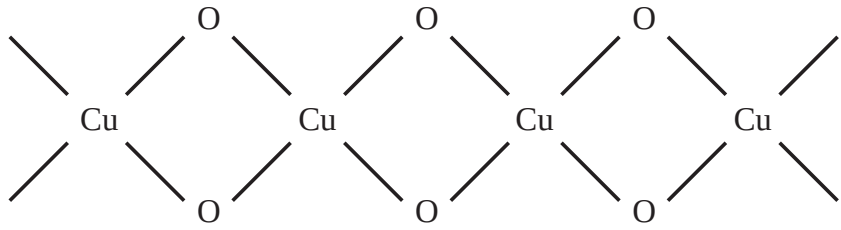

Fig. 5.24. The main structural motive of several compounds containing Cu^{2+} coupled by the 90° Cu–O–Cu superexchange path

$x^2 - y^2$-like orbitals of Cu give rise to a (weak) ferromagnetic interaction. This is seen, in particular, in the "telephone number" compound $Ca_{14}Cu_{24}O_{41}$, in which spin ladders coexist with the spin chains having the structure of Fig. 5.24, and the exchange in these chains is known to be ferromagnetic.

Finally the compound $CuGeO_3$ with a similar structure may be mentioned: this is the first inorganic material showing a spin-Peierls transition. The angle Cu–O–Cu is slightly larger than 90° ($\sim 98°$) but is not enough to make the exchange antiferromagnetic (as is needed for the spin-Peierls transition). This presents a formidable problem, and special physical mechanisms are needed to overcome the second GKA rule and make the exchange antiferromagnetic [17].

5.7 Exchange Mechanism of Orbital Ordering

As discussed previously, even with a fixed lattice, superexchange leads not only to magnetic, but also to orbital ordering [18,6]. In Sect. 5.3 the Jahn–Teller theorem, the lifting of the orbital degeneracy and the resulting orbital ordering, the distortion of the lattice and the effective intersite interaction due to this mechanism was discussed. The general ideas developed in Sect. 5.6 will be applied to a particular question: what are the possible mechanisms of orbital ordering in systems with orbitally degenerate (Jahn–Teller) ions.

In order to shed light on this question, as shown in Fig. 5.25, imagine two neighbouring TM ions with one electron on each, occupying doubly-degenerate orbitals. Suppose for simplicity that only diagonal hoppings are allowed: those

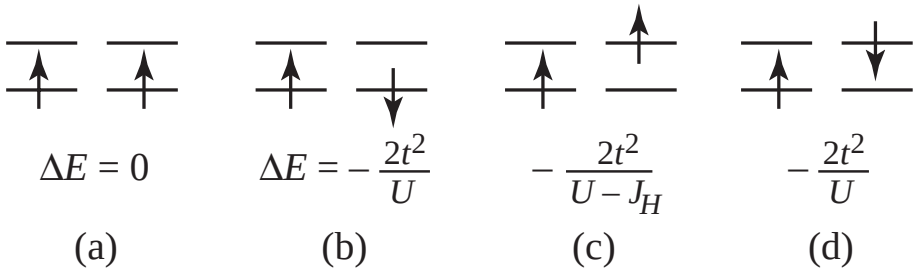

Fig. 5.25. The scheme illustrating the tendency to simultaneous spin and orbital ordering due to superexchange mechanism for a doubly-degenerate orbitals

between orbitals 1 in a nn state and those between orbitals 2: $t^{11} = t^{22} = t$, $t^{12} = 0$. If the arguments are generalized as shown in Figs. 5.15 and 5.21, the energy gain due to virtual hopping of electrons onto neighbouring sites can easily be calculated (as shown in Fig. 5.25). Immediately it can be seen that due to the influence of the Hund's rule interaction (which decreases the energy of the intermediate state with two parallel spins), the state of Fig. 5.25c is favoured. Thus, whereas for the nondegenerate case of Fig. 5.15 the superexchange leads to an antiferromagnetic spin interaction, here the state with both the spin and orbital ordering is stabilized; in this particular case the one with the ferromagnetic spin ordering and "antiferro-orbital" one.

Again this treatment can be made rigourous and the effective exchange Hamiltonian in contrast to (5.7), would contain terms $\boldsymbol{S}_i\boldsymbol{S}_j$, terms describing orbital ordering $\tau_i\tau_j$ and terms describing the coupling of the spin and orbital degrees of freedom of the form $S_iS_j \cdot \tau_i\tau_j$.

Due to the complicated shape of real e_g-functions the actual form of the resulting effective Hamiltonian for real systems is also much more complex [18], but the main qualitative conclusions are similar: even with a fixed lattice (without real electron–lattice interaction usually invoked to explain cooperative Jahn–Teller ordering), in purely electronic terms the exchange interactions may cause both the magnetic (spin) and orbital (Jahn–Teller) ordering. One can even speak

here about the "Jahn–Teller ordering without Jahn–Teller interaction". It should be noted that in this mechanism the orbital and magnetic orderings are strongly interrelated (although they can in general occur at different temperatures).

An interesting and important question arises as to the dominant mechanism leading to orbital ordering in real materials. Of course, generally speaking, both mechanisms (via electron–lattice interaction and via exchange interaction) are present simultaneously. Usually they both lead to the same orbital structure, so that experimentally it is very difficult to separate the contribution of different mechanisms. Novel possibilities to resolve this problem appeared recently with the development of a new calculation technique, the LDA + U method [19], which gives the possibility to obtain orbitally ordered structures by either fixing the undistorted lattice or taking into account the real lattice distortion. These calculations can be visioned as "numerical experiments" which permit to isolate the purely electronic contribution from the lattice one.

The experience gained so far [20] shows that indeed, correct orbital structures can be obtained even by fixing a symmetric lattice. A comparison of the energies from corresponding solutions shows that about 60–70% of the total energy gain due to the orbital ordering is provided by the electronic (exchange) contribution, the remaining 30–40% being gained when the lattice is released and permit to relax to a new equilibrium position corresponding to the correct orbital occupation. Thus from these calculations we can indeed conclude that the electronic (exchange) contribution gives at least a comparable, but maybe even dominant, contribution to the orbital ordering, as compared to the usually invoked electron–lattice interaction (although the latter is definitely also important).

5.8 Doping of Magnetic Insulators; Double Exchange

Up to now we have dealt exclusively with magnetic insulators with an integer number of electrons per TM ion. In this section the general case of doping (i.e. changing the average occupation of the *d*-levels) in magnetic insulators will be discussed.

A number of intriguing phenomena may be seen when doping: such as the coexistence of different valence states of a TM e.g. magnetite Fe_3O_4 (formally Fe^{2+} and Fe^{3+} ions) or NaV_2O_5 (V^{4+} and V^{5+}). The different valence states can order ("crystallize") in the material, giving a charge-ordered (CO) state; usually these CO states are insulating. However, there may be situations when rapid exchange, or hopping, of electrons between different ions exists.

In contrast with Mott insulators with an integer number of electrons, here the hopping does not in general require any extra excitation energy and can occur quite freely, giving rise to a metallic conductivity. Thus a metallic state can be obtained with its magnetic properties differing strongly from the parent insulating compounds. Typically a ferromagnetic (or at least "more ferromagnetic") spin arrangement is obtained.

This phenomenon not only exists in doped or mixed-valence compounds, but also in oxides with integer valence. If there is a large enough electron hopping t and corresponding bandwidth W ($\sim t$) and if $W \gtrsim U$, a metallic state will be obtained. Sometimes these states behave magnetically as Pauli paramagnets (possibly with exchange enhancement) as in $LaNiO_3$. But in other systems of this type, especially those with small or negative charge-transfer gap (see Sect. 5.5), the corresponding metallic state is still characterized by strong electron correlations. In these cases magnetic ordering in such metallic states may exist; again usually a ferromagnetic one is seen. This is the case in $SrFeO_3$ or $SrCoO_3$.

For the rest of this section we will discuss the origin of ferromagnetism in doped Mott insulators. The most popular example of such a system nowadays is provided by doped $LaMnO_3$, e.g. $La_{1-x}Sr_xMnO_3$, where with increasing x we go from the insulating state with A-type (layered) antiferromagnetism via a complicated intermediate state (its exact nature is not known, see below) to a ferromagnetic state for $x \gtrsim 0.18$. It is this last state which displays the property of Colossal Magnetoresistance (CMR) and which attracts now such attention.

The basic concept used to explain the appearance of ferromagnetism in these systems and its interplay with the metallic conductivity is through the double exchange model, first developed by Zener [21], later put on firm theoretical grounds by Anderson and Hasegawa [22] and by De Gennes [23]. See textbooks and review articles [5,7] for a detailed description; we give here only the general scheme without any details which can be found in these reviews.

The general idea for CMR is as follows. Suppose a lattice of localized electrons, and add a certain (small) number of extra electrons or holes which can in principle propagate through the crystal but these may also interact with the background of localized spins. For the system $La_{1-x}Sr_xMnO_3$ our initial ionic state for $x = 0$ is $Mn^{3+}(t_{2g}^3 e_g^1)$, and by substituting La by Sr we remove x electrons, i.e. create x holes in the e_g-band (or create x $Mn^{4+}(t_{2g}^3)$ ions).

It may be easier to visualize (although more difficult to prepare experimentally) the opposite situation: start with the material $CaMnO_3$ containing $Mn^{4+}(t_{2g}^3)$ ions with three localized t_{2g}-electrons (the spin of such ions is $S = \frac{3}{2}$), and dope it with a rare earth, e.g. Sm^{3+}: by this we add a certain number of d-electrons in e_g-levels which in general can form a narrow band.

Such electrons in general can indeed move through the crystal (if we ignore the potential of the impurity itself, all the positions of the extra electron are equivalent). But if magnetic order of the background localized spins exists, it can influence and maybe hinder the motion of doped charge carriers.

$CaMnO_3$ is known to have a two-sublattice (G-type) antiferromagnetic ground state in which all the nearest neighbours of a given site have spins opposite to it. However, in $CaMnO_3$ a strong Hund's rule coupling exists between d-electrons, which (classically) forces the extra electron to have its spin parallel to the localized spin of the site. As a result the situation shown in Fig. 5.26 will take place: an extra electron at the site i should have spin up, but it cannot hop to the neighbouring site j having spin down.

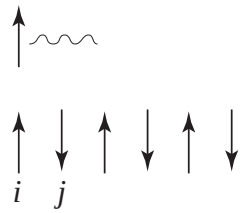

Fig. 5.26. An illustration of why the antiferromagnetic ordering hinders the motion of an extra electron in case of strong Hund's rule coupling

If localized spins are treated classically, it can be shown that for strong Hund's rule exchange $J_H > t$ (where t is the hopping matrix element of the extra electron) the *effective* hopping is reduced,

$$t_{ij} \longrightarrow t_{\mathit{eff}} = t \cos \frac{\theta_{ij}}{2} \tag{5.12}$$

where θ_{ij} is the angle between spins of the sites i and j. Thus for purely antiferromagnetic ordering $\theta_{ij} = \pi$, and $t_{\mathit{eff}} = 0$. On the other hand, if the system is made *ferromagnetic*, $\theta_{ij} = 0$, the electrons can move freely, $t_{\mathit{eff}} = t$.

The electrons hopping from site to site with the matrix element t_{eff} (5.12) would form a band, with the spectrum (e.g. in cubic lattice)

$$\varepsilon(k) = -2t_{\mathit{eff}}(\cos k_x + \cos k_y + \cos k_z) \tag{5.13}$$

and a (small) number of doped electrons would occupy the states at the bottom of this band near $\varepsilon_{min} = -6t_{\mathit{eff}}$. Thus whereas in the undoped materials, as assumed, the system is antiferromagnetic due to the corresponding exchange interaction of localized (here t_{2g}) spins J, in the doped system a gain in energy (kinetic energy of the doped carriers) by increasing t_{eff} can be obtained, i.e. by making the system "more ferromagnetic".

If now we assume that two sublattices form a canted structure with the angle between sublattices θ, the total energy (per site) as a function of this angle may be written in the quasiclassical approximation as

$$E(\theta) = JS^2 \cos\theta - 6tx \cos\frac{\theta}{2}\,. \tag{5.14}$$

(Here we took into account the relations (5.7), (5.12), and assumed that x is small so that all the electrons are at the bottom of corresponding band.) The minimisation of the energy (5.14) in θ gives

$$\cos\frac{\theta}{2} = \frac{3}{2}\frac{t}{JS^2}x\,, \tag{5.15}$$

i.e. under the influence of doping (increasing x) the original antiferromagnetic structure becomes *canted*, see Fig. 5.27, i.e. there will coexist both antiferromagnetic and ferromagnetic components of the magnetic order.

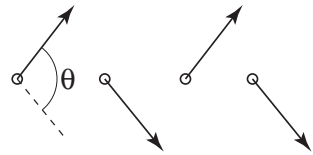

Fig. 5.27. The canted antiferromagnetic structure, with the antiferromagnetic component $\pm S^z = \pm S \sin\theta/2$ and the ferromagnetic one $S_x = S\cos\theta/2$

With increasing x the canting angle θ would decrease and for

$$x > x_c = \frac{2}{3}\frac{JS^2}{t} \tag{5.16}$$

the magnetic order would become purely *ferromagnetic*. This is the standard explanation for the change of the magnetic structure with doping. It is used for example for the description of the appearance of ferromagnetism *together with the metallic conductivity* in doped manganites.

There are many subtle points in this model. First of all, even in this quasiclassical treatment, taking result (5.11) we cannot yet say that the resulting magnetic structure would be a two-sublattice canted antiferromagnetic one. Only the local pitch angle θ_{ij} is fixed by this treatment; one can however imagine an alternative magnetic structure, e.g. the helicoidal one, with the same pitch angle.

More important may be the neglect of quantum effects in the above treatment. The "ferromagnetic" on-site Hund's rule coupling does not necessarily require the spins of the extra electron and of localized spins to be parallel, as in Fig. 5.26. These should form a state with *maximum total spin*, e.g. a triplet state of the localized spin $s = \frac{1}{2}$, but this triplet can have a total z-projection 0, $\frac{1}{\sqrt{2}}(1\uparrow 2\downarrow + 1\uparrow 2\downarrow)$. It can be shown [24,25] that the motion of the extra electron is quantum-mechanically possible even on a purely antiferromagnetic background, albeit with a reduced bandwidth. The account of these factors modifies the resulting phase diagram, leading e.g. to the appearance of a lower critical concentration x_{c1} [25] below which the original antiferromagnetic structure is undistorted.

But probably the most "dangerous" point in this treatment is the assumption of spatial homogeneity of the system. Using formulae (5.14) and (5.16) the total energy of the assumed homogeneous canted state can be calculated with the minimum energy being

$$E(x) = -JS^2 - \frac{9}{2}\frac{t^2}{JS^2}x^2\,. \tag{5.17}$$

However, in this state the compressibility $\kappa^{-1} \sim d^2E/dx^2$ is *negative* [25] which indicates an absolute instability of such a state towards phase separation, i.e. creation of a state with an inhomogeneous distribution of both the extra charge carriers and magnetic order. For instance, the ferromagnetic metallic "droplets" may be formed in an antiferromagnetic insulating matrix [25].

A detailed analysis of the resulting state requires also an account of the long-range Coulomb interaction and lattice distortion; in addition in real manganites of the change of orbital ordering etc., and this is still not a tractable problem. However, generally speaking the creation of a spatially inhomogeneous state in lightly doped manganites, with the properties (e.g. in transport) of percolation systems should be expected and only at higher doping level the (more) homogeneous metallic and ferromagnetic state can be obtained, although some inhomogeneity can still be present.

Doped manganites can be connected to a specific feature of orbital degeneracy of e_g-levels or e_g-bands in which mobile electrons reside [26]. Probably this is relevant for an interesting and not yet completely understood asymmetry in the behaviour of doped manganites with $x > 0.5$ and $x < 0.5$. Whereas for overdoped manganites ($x > 0.5$) a very stable insulating state with regular stripe structure is formed, for $x < 0.5$ a ferromagnetic metallic state is obtained.

5.9 Concluding Remarks

In this short review the basic physical factors determining the electronic and magnetic structure of magnetic oxides were explained. Of course, this chapter cannot substitute a real textbook, but the main physical factors and mechanisms determining the type of magnetic ordering and its interplay with the insulating or metallic behaviour of corresponding materials were stressed.

There are always a lot of specific details important for particular materials. All these details, however, do not invalidate the general conclusion that, generally speaking, antiferromagnetism exists typically in insulating materials, and ferromagnetism is associated with metallic conductivity. There are of course some exceptions to this rule, i.e. there exist ferromagnetic insulators, but these are rare exceptions, and usually a special explanation is required, for further details see the discussion in [7]. The general trend is the one formulated above: antiferromagnetism prefers to coexist with the insulating state, and ferromagnetism with the metallic one. The underlying mechanism responsible for this trend is due to *virtual* hopping of electrons typically giving rise to a superexchange-generated antiferromagnetism, whereas *real* motion of electrons stabilizes ferromagnetism by the double-exchange mechanism. This strong interplay between magnetic structure and transport properties makes these systems so interesting and promising for possible applications in spin electronics.

References

1. J. M. D. Coey, M. Viret, and S. von Molnar, Adv. Phys. **48**, 167 (1999).
2. Y. Shapira, S. Foner, R. L. Aggarwal, and T. B. Read, Phys. Rev. B **8**, 2316 (1973).
3. J. B. Goodenough, "Magnetism and chemical bond," Interscience Publ., N.Y.-Lnd., 1963.
4. A. Abraham and B. Bleney, "Electron paramagnetic resonance of transition ions," Clarendon Press, Oxford 1970.

5. P. W. Anderson, in "Solid State Physics", ed. H. Ehrenreich, F. Seitz, and D. Turnbull, Academic Press, N.Y. 1963, vol. 14, p. 99.
6. K. I. Kugel and D. I. Khomskii, Sov. Phys.—Uspekhi **25**, 231 (1982).
7. D. Khomskii and G. Sawatzky, Solid State Comm. **102**, 87 (1997).
8. M. A. Korotin, S. Yu. Ezhov, I. V. Solovyev, V. I. Anisimov, D. I. Khomskii, and G. A. Sawatzky, Phys. Rev. B **54**, 5309 (1996).
9. R. Englman, "The Jahn-Teller effect in molecules and crystals", Wiley–Interscience, Lnd.–N.Y. 1972.
10. M. Kaplan and B. Vekhter, "Cooperative phenomena in Jahn-Teller crystals", Plenum Press, 1995.
11. N. F. Mott, "Metal–Insulator transitions", Taylor and Francis, London 1974.
12. D. I. Khomskii, The Phys. of Metals and Metallography, **29**, 31 (1970).
13. P. W. Anderson, Phys. Rev. **115**, 2 (1959).
14. J. Zaanen, G. A. Sawatzky, and J. Allen, Phys. Rev. Lett. **55**, 418 (1985).
15. D. Khomskii, Lithuanian Journal of Physics, **37**, 65 (1997).
16. M. A. Korotin, V. I. Anisimov, D. I. Khomskii, and G. A. Sawatzky, Phys. Rev. Lett. **80**, 4305 (1997).
17. W. Geertsma and D. Khomskii, Phys. Rev. B **54**, 3011 (1996).
18. K. I. Kugel and D. I. Khomskii, Sov. Phys.—JETP **37**, 725 (1973).
19. V. Anisimov, A. Aryasetiawan, and A. Lichtenstein, J. Phys. C: Condens. Matter **9**, 767 (1997).
20. A. Lichtenstein, V. Anisimov, and J. Zaanen, Phys. Rev. B **52**, R5467 (1995).
21. C. Zener, Phys. Rev. **81**, 403 (1951).
22. P. W. Anderson and H. Hasegawa, Phys. Rev. **100**, 675 (1955).
23. P. G. De Gennes, Phys. Rev. **118**, 141 (1960).
24. E. L. Nagaev, Sov. Phys.—Uspekhi **166**, 833 (1996).
25. M. Kagan, D. Khomskii, and M. Mostovoy, Eur. Phys. J. B **12**, 217 (1999).
26. J. van den Brink and D. Khomskii, Phys. Rev. Lett. **82**, 1016 (1999).